

Heat Capacity Measurements of Extremely Thin Substrate-Free Liquid-Crystal Films¹

T. Stoebe,² J. T. Ho,³ and C. C. Huang^{2,4}

A state-of-the-art calorimetric system has been established. The system enables us to measure simultaneously heat capacity and optical reflectivity of free-standing liquid-crystal films from many hundreds down to only two molecular layers in thickness. Our experimental results on the smectic-A-hexatic-B and smectic-C-smectic-I transitions cannot be described solely in terms of the creation of bond-orientational order, indicating that additional molecular order must be present in the hexatic phases of liquid crystals.

KEY WORDS: calorimeter; density; film; heat capacity; hexatic; liquid crystal; smectic-A-hexatic-B transition; two-dimensional melting.

1. INTRODUCTION

For many decades, heat capacity data have revealed numerous important physical properties, e.g., phononic and electronic properties of crystalline materials, the fundamental excitations of amorphous materials at low temperatures, the existence of an energy gap in the superconducting state, and the nature of a large number of phase transitions. In many circumstances, heat capacity is the most (and in some, the only) experimentally accessible quantity related to a second derivative of the free energy and to the divergent behavior near a phase transition. Consequently, heat capacity measurements have been vital in the effort to understand the nature of various phase transitions. As an important example, heat capacity data have allowed different packing arrangements of monolayers of molecules of

¹ Paper presented at the Twelfth Symposium on Thermophysical Properties, June 19–24, 1994, Boulder, Colorado, U.S.A.

² School of Physics and Astronomy, University of Minnesota, Minneapolis, Minnesota 55455, U.S.A.

³ Department of Physics, State University of New York, Buffalo, New York 14260, U.S.A.

⁴ To whom correspondence should be addressed.

rare gases adsorbed on graphite to be distinguished [1]. The heat capacity anomaly from ^4He /graphite foam at the order-disorder transition and critical coverage yields the critical exponent $\alpha = 0.28$. This value of α implies the existence of a $(3 \times 3) R30^\circ$ structure of monolayer ^4He on bare graphite with a three-state Potts symmetry. On the other hand, the logarithmic temperature variation of heat capacity near the order-disorder transition of ^4He adsorbed on Kr-plated graphite indicates the existence of a $(1 \times 1) [1/2]$ triangular structure on a honeycomb lattice of adsorption sites. In this case, therefore, the system belongs to the two-dimensional Ising universality class.

Soon after remarkable theoretical advances introduced a novel melting mechanism and predicted the existence of an intermediate phase between the liquid and the solid phases in two dimensions (2D) [2], Pindak et al. [3] discovered a unique liquid-crystal mesophase below the smectic-A phase of 650BC. 650BC is a member of the *nm*OBC [*n*-alkyl-4'-*n*-alkoxybiphenyl-4-carboxylate] homologous series. Based on the x-ray diffraction data, this intriguing mesophase exhibits long-range bond-orientational order (namely, hexatic order) but only short-range positional order. It has been named the hexatic-B (HexB) phase and is often characterized as a three-dimensional stack of the two-dimensional hexatic phase as suggested by Birgeneau and Litster [4]. The fact that both the SmA and the HexB phases, as well as their tilted counterparts [smectic-C (SmC) and smectic-I (SmI)], possess a layered structure allows the preparation of free-standing liquid-crystal films in these phases. The free-standing films are suspended around a hole cut into a film plate, much like a soap film is suspended on a ring. By choosing appropriate liquid-crystal compounds, uniform free-standing films with thicknesses ranging from only two to a few hundred molecular layers can be easily prepared.

The existence of hexatic order in liquid crystals has been further confirmed by detailed electron diffraction studies of the HexB phase in thin 650BC films [5] and x-ray diffraction investigations of the SmI phase in thick 8OSI films [6]. 8OSI refers to the compound 4-(2'-methylbutyl)phenyl-4'-*n*-octyloxybiphenyl-4-carboxylate. In addition to the remarkable structural information obtained from such diffraction probes, calorimetric measurements on bulk samples yield clear thermodynamic signatures related to the SmA-HexB-CryE (crystal-E) and SmC-SmI-CryJ (crystal-J) transitions. These phase sequences represent 3D realizations of the 2D liquid-hexatic-solid transition sequence introduced in the novel theories of 2D melting mentioned above.

By utilizing a number of experimental techniques for structural identification, the novel hexatic phase has also been reported in various other 2D systems [7]. However, to date, only liquid-crystal system (in the form

of stacked three-dimensional phases) have provided the essential thermodynamic signature of a phase transition into a liquid-like higher temperature phase or a solid-like lower temperature phase. Three critical exponents ($\alpha = 0.60$, $\beta = 0.19$, and $\eta = -0.21$) have been found to characterize the continuous SmA–HexB transition exhibited by members of the *nm*OBC homologous series. These values satisfy the following scaling relations in three dimensions ($d = 3$): $d\nu = 2 - \alpha$, $2\nu - \eta\nu = 2 - 2\beta - \alpha$. However, this set of critical exponents is very different from those ($\alpha = -0.013$, $\beta = 0.35$, and $\eta = 0.04$) of the 3D XY universality class or those ($\alpha = 1/2$, $\beta = 1/4$, and $\eta = 0$) near a tricritical point. The experimental results, therefore, strongly demonstrate that the (XY symmetric) hexatic order identified by diffraction studies is not sufficient to describe the nature of the SmA–HexB transition in bulk liquid crystals. As a result, we have suggested that this intriguing transition may belong to a new universality class [7, 8].

It is now well-known that systems in the XY symmetry class may exhibit a unique topological defect-mediated transition in two dimensions which is very different from ordinary order–disorder transitions. Instead of the divergent behavior found near most continuous order–disorder transitions, only an essential singularity exists near the topological defect-mediated transition temperature (T_{dm}). This weak temperature dependence is reflected in the very broad heat-capacity hump, due to the massive dissociation of bound topological defects, which is expected to be present on the high-temperature side of T_{dm} [9]. To test our hypothesis related to a new universality class, we have undertaken the measurement of the heat capacity of extremely thin liquid-crystal films near the SmA–HexB transition of *nm*OBC compounds. Because the hexatic order parameter is XY-like, sufficiently thin films could be expected to exhibit a broad heat-capacity hump characteristic of a defect-mediated transition through the SmA–HexB transition. Successful measurement of the temperature dependence of the heat capacity of such thin films is not an easy task. This point can be easily illustrated by realizing that there is only about 500 ng of liquid-crystal material in a 1-cm diameter, two-layer film (25 Å/layer). Our effort, therefore, has required a number of technical improvements necessary to achieve this seemingly impossible goal.

2. EXPERIMENTAL SETUP

Employing a number of ideas, we have now established a state-of-the-art calorimetric system which enables us to measure simultaneously heat capacity and optical reflectivity from free-standing liquid-crystal films with thicknesses ranging from two to a few hundred molecular layers. Details of our systems have been published elsewhere [10–12]. Figure 1 presents a

schematic diagram and the key concepts of our experimental geometry. To provide the AC heat source necessary for the calorimetric measurements, we mechanically modulate (at 42 Hz) the infrared radiation ($3.39 \mu\text{m}$) from a He-Ne laser placed inside a temperature-regulated aluminium housing. The free-standing films are prepared over a 1-cm-diameter hole cut into a stainless-steel plate which is placed inside a temperature-controlled oven. At the 42-Hz chopping frequency, the $1/2$ -atm argon exchange gas inside the oven has a thermal diffusion length $l_d = 0.6 \text{ mm}$. Two tiny thermocouple junctions (separated 5 mm) made of $12\text{-}\mu\text{m}$ -diameter, type-E thermocouple wires are placed below the film, directly in the path of the laser radiation. In the case of thin films, while both thermocouple junctions are exposed to the transmitted $3.39\text{-}\mu\text{m}$ radiation at 42 Hz, the film thermocouple, located only $25 \mu\text{m}$ below the film, experiences an additional temperature oscillation contribution due to the film. Operating a lock-in amplifier in a differential mode between the signals from these two thermocouple junctions enables us to detect the magnitude of the film temperature oscillation. This temperature oscillation is directly related to the heat capacity of the film.

Another intensity-stabilized He-Ne laser operating at $0.638 \mu\text{m}$ is employed as the light source for the reflectivity measurement. To facilitate lock-in detection of both signals, the $0.638\text{-}\mu\text{m}$ radiation is chopped at a much higher frequency (675 Hz). A small fraction of the beam is split off to a monitor. The majority of the beam is focused and directed so that it intersects the film at near-normal incidence with a $1/e^2$ width of approximately $300 \mu\text{m}$. The reflected and monitor beams are detected using similar photovoltaic detectors and another lock-in amplifier operating in the differential mode. Great care was exercised to ensure that the

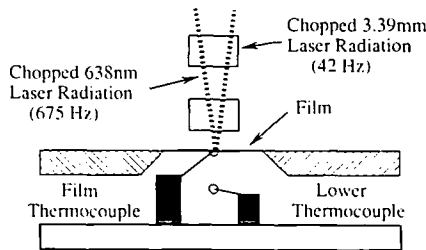


Fig. 1. Schematic diagram displaying the experimental system for the simultaneous heat capacity and optical reflectivity measurements. The calorimetric measurement employs $3.39\text{-}\mu\text{m}$ laser radiation as an AC heat source, while the focused $0.64\text{-}\mu\text{m}$ radiation is utilized as the light source for the reflectivity measurement.

calorimetric and optical reflectivity signals were obtained from the same portion of the film while avoiding direct heating of the tiny thermocouple junctions below the film by the $0.638\text{-}\mu\text{m}$ radiation. The system currently operates with resolution better than a few parts in 10^5 for both probes.

3. RESULTS AND DISCUSSION

By considering the thin films to be thin dielectric slabs and making a few reasonable assumptions, one can obtain in-plane density from the optical reflectivity data. The temperature variation of the heat capacity (C_p) and in-plane density (ρ_Λ) data simultaneously obtained from a two-layer 3(10)OBC film near the SmA–HexB transition are shown in Fig. 2. It should be noted that, because of the fairly small thermal diffusion length of the argon exchange gas at our chopping frequency, only a small portion ($\approx 0.6\text{-mm}$ diameter) of the film is actually probed by our calorimetric system (see Fig. 1). *Thus, the amount of the sample actually contributing to our heat capacity measurement from a two-layer film is less than 20 ng!*

In thicker *nm*OBC films ($N > 2$ layers), more than one heat capacity peak associated with the SmA–HexB transition can be resolved [11, 13]. This phenomenon can be understood as a novel series of surface-enhanced layer-by-layer transitions [14, 15]. Because thicker films clearly exhibit effects dependent on relative position within the film, only two-layer films (exhibiting a single heat-capacity peak) can be categorized as two-dimensional systems. So far, more than 4000 thin *nm*OBC films have been prepared in our laboratories; we have not yet observed a one-layer film. Unlike the theoretical prediction, the heat capacity anomaly due to the two-layer 3(10)OBC film shown in Fig. 2 is clearly quite sharp. The data, therefore, appear much more like a standard order–disorder transition than defect-mediated. At the peak position of the heat capacity anomaly, the in-plane density data display a sign change in curvature. Because of the high resolution of the in-plane density data, a meaningful temperature derivative can be obtained. Within our experimental resolution, $d\rho_\Lambda/dT$ is proportional to C_p and the two data sets can be scaled to overlap [12]. This scaling has allowed us to conduct a simultaneous fit of both heat capacity and in-plane density data to the following two equations:

$$C_p = A^\pm |t|^{-\alpha} + B_1 \quad (1)$$

and

$$\rho_\Lambda(T) = \rho_\Lambda(T_c) + (B_1 - E) T_c t/D + T_c A^\pm |t|^{1-\alpha}/[D(1-\alpha)] \quad (2)$$

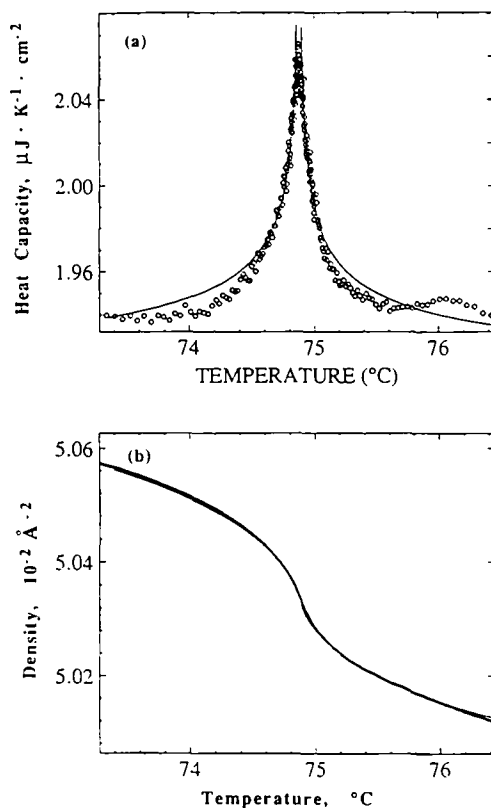


Fig. 2. Heat capacity (a) and in-plane molecular density (b) data near the SmA-HexB transition of a two-layer 3(10)OBC film. The data were obtained from the simultaneous measurement of both heat capacity and optical reflectivity. The results from simultaneously fitting the heat capacity and in-plane density data to Eqs. (1) and (2), respectively, are displayed as solid lines.

Here B_1 is the background heat capacity contribution and the constants D and E could be determined from the scaling of the $d\rho_A/dT$ data onto the heat capacity data, so that $C_p = Dd\rho_A/dT + E$. With T_c held fixed at the peak position of the heat capacity anomaly, only four parameters (B_1 , A^+ , A^- , and α) are therefore necessary to fit simultaneously both the heat capacity and the in-plane density data. The fitting results are quite satisfactory over more than one and a half decades in reduced temperature and are included in Fig. 2 as the solid lines. The important fitting parameters are $\alpha = 0.31 \pm 0.03$ and $A^+/A^- = 0.93 \pm 0.07$. Because the heat capacity

anomaly can be well described by a power law, these results clearly demonstrate the inadequacy of simple bond-orientational order as the relevant order parameter for this transition. It is important to note that the transition into a three-state Potts system in 2D is characterized by $\alpha = 1/3$, quite close to the exponent obtained above.

Because the molecular-tilt order is expected to couple to the bond-orientational order, hexatic domain problems can be avoided in the tilted phases. The nature of the hexatic order in the tilted hexatic phases has therefore been studied in considerably greater detail than in the HexB phase. Detailed x-ray diffraction data suggest that the bond-orientational order (with the XY symmetry) is the primary order parameter and is sufficient to describe the nature of the SmC–SmI transition [6]. To ensure that our experimental results on the SmA–HexB transition do not represent a singular exception, we [16] have conducted detailed calorimetric investigations near the SmC–SmI transition of two-layer films of DOBAMBC [*p*-decyloxybenzylidene-*p*-amino-2-methylbutyl cinnamate]. The data are surprisingly similar to the SmA–HexB case, and although the x-ray results indicate that bond-orientational order is important, it is, again, not sufficient to describe the nature of the transition. *Therefore, a simple hexatic phase exhibiting the thermodynamic signature of a phase transition into either the liquid or the solid phase remains to be identified in nature.*

Our calorimetric results on two-layer 3(10)OBC films near the SmA–HexB transition require the existence of some additional molecular order aside from the observed bond-orientational order. To provide direct support of this conclusion, we have conducted electron diffraction studies to search for such additional order. Utilizing a long exposure time, an overexposed diffraction pattern from an eight-layer 3(10)OBC film in the HexB phase was obtained. It is displayed in Fig. 3. Besides the six-fold arcs indicative of bond-orientational order, Fig. 3 exhibits 12 additional weak, but discernible, diffraction spots, at locations which are characteristic of a herringbone molecular order [3]. A high-resolution x-ray diffraction study is necessary to determine the extent (pseudo-long-range or short-range order) of this herringbone molecular order. The observation of herringbone order is important because it can be described by a three-state Potts hamiltonian, which exhibits a sharp heat-capacity anomaly in 2D. We have since conducted Monte Carlo simulation experiments to confirm that it is possible to establish simultaneously both bond-orientational order and herringbone order through a continuous transition in 2D. The simulation exhibits a sharp heat-capacity anomaly that can be characterized by a critical exponent, $\alpha \approx 1/3$ [17]. Continued simulation work in both 2D and 3D is in progress.



Fig. 3. Electron diffraction pattern from an eight-layer 3(10)OBC film. The plate was purposely overexposed (several minutes instead of several seconds) to reveal the 12 weak, but discernible, herringbone diffraction spots.

In conclusion, not only have we established an extremely sensitive calorimetric system to measure the heat capacity and in-plane density of extremely thin free-standing liquid-crystal films, but also we have demonstrated that detailed calorimetric data can provide crucial structural information which may escape other experimental investigations.

ACKNOWLEDGMENTS

This work was supported in part by the Donors of the Petroleum Research Fund, administered by the American Chemical Society and by the National Science Foundation, Solid State Chemistry, Grants DMR 93-00781 and DMR 91-03921. One of us (T.S.) would like to acknowledge support from IBM.

REFERENCES

1. M. J. Tejwani, O. Ferreira, and O. E. Vilches, *Phys. Rev. Lett.* **44**:152 (1980).
2. B. I. Halperin and D. R. Nelson, *Phys. Rev. Lett.* **41**:121, (1978); D. R. Nelson and B. I. Halperin, *Phys. Rev. B* **19**:2457 (1979).
3. R. Pindak, D. E. Moncton, S. C. Davey, and J. W. Goodby, *Phys. Rev. Lett.* **46**:1135 (1981).
4. R. J. Birgeneau and J. D. Litster, *J. Phys. Lett. (Paris)* **39**:399 (1978).
5. M. Cheng, J. T. Ho, S. W. Hui, and R. Pindak, *Phys. Rev. Lett.* **61**:550 (1988).
6. J. D. Brock, A. Aharony, R. J. Birgeneau, K. W. Evans Lutterodt, J. D. Litster, P. M. Horn, G. B. Stephenson, and A. R. Tajbakhsh, *Phys. Rev. Lett.* **57**:98 (1986).
7. C. C. Huang and T. Stoebe, *Adv. Phys.* **42**:343 (1993).
8. G. Nounesis, R. Geer, H. Y. Liu, C. C. Huang, and J. W. Goodby, *Phys. Rev. A* **40**:5468 (1989).
9. S. A. Solla and E. K. Riedel, *Phys. Rev. B* **23**:6008 (1981).

10. R. Geer, T. Stoebe, T. Pitchford, and C. C. Huang, *Rev. Sci. Instrum.* **62**:415 (1991).
11. R. Geer, T. Stoebe, and C. C. Huang, *Phys. Rev. E* **48**:408 (1993).
12. T. Stoebe, C. C. Huang, and J. W. Goodby, *Phys. Rev. Lett.* **68**:2944 (1992).
13. R. Geer, T. Stoebe, C. C. Huang, R. Pindak, J. W. Goodby, M. Cheng, J. T. Ho, and S. W. Hui, *Nature* **355**:152 (1992).
14. T. Stoebe, R. Geer, C. C. Huang, and J. W. Goodby, *Phys. Rev. Lett.* **69**:2090 (1992).
15. T. Stoebe, A. J. Jin, P. Mach, and C. C. Huang, *Int. J. Thermophys.*, in press.
16. T. Stoebe and C. C. Huang, *Phys. Rev. E (RC)* **50**:R32 (1994).
17. I. M. Jiang, S. N. Huang, J. Y. Ko, T. Stoebe, A. J. Jin, and C. C. Huang, *Phys. Rev. E (RC)* **48**:3240 (1993).